

A carbon–nitrogen complex in gallium phosphide

W. Ulrici

Paul-Drude-Institut für Festkörperelektronik, Hausvogteiplatz 5-7, 10117 Berlin, Germany

B. Clerjaud

Institut des NanoSciences de Paris-UMR CNRS 7588, Université Pierre et Marie Curie, 140 rue de Lourmel, 75015 Paris, France

(Received 31 March 2005; published 7 July 2005)

In gallium phosphide containing nitrogen ($[N_p] > 10^{17} \text{ cm}^{-3}$) and carbon ($[C_p] > 10^{16} \text{ cm}^{-3}$) a sharp local vibrational mode at 2087.12 cm^{-1} at $T=7 \text{ K}$ is observed. It is shown that the complex responsible for this local vibrational mode is a carbon–nitrogen complex; the carbon–nitrogen bond is a triple bond aligned along the $\langle 001 \rangle$ axes of the lattice. A microscopic structure of the complex is proposed. It is suggested that the equivalent complex exists in GaAs and is characterized by a local vibrational mode at 2088.50 cm^{-1} at $T=7 \text{ K}$. The carbon atoms involved in these complexes do not contribute to the carbon p -type doping of the crystals.

DOI: [10.1103/PhysRevB.72.045203](https://doi.org/10.1103/PhysRevB.72.045203)

PACS number(s): 61.72.Vv, 63.20.Pw, 78.30.Fs

I. INTRODUCTION

There is presently a great interest in dilute III-V nitrides. The presence of few percent of nitrogen changes the band gap of III-V materials drastically. Dilute quaternary nitrides have demonstrated the singular properties of being tunable continuously in both gap and lattice parameter simply by adjusting the composition.¹ This opens the possibility, in principle, to adjust the band gap of the material remaining lattice matched to Si.² However, despite the huge potential advantages of these materials and the large amount of work performed on them, the realization of devices based on these materials is still scarce. This is due mostly to the presence of uncontrolled defects in the III-V-N dilute nitrides. The investigation of defects in these materials is therefore a topic of importance.³ The investigation of defects in III-V-N dilute nitrides is quite complex. This is due to the fact that these materials are usually epitaxial layers that are most often strained because of the lattice mismatch with the substrate. Strain, together with alloying effects lead to a broadening of the spectroscopic features and complicate the interpretation of the data. In order to overcome these drawbacks and to allow experiments under uniaxial stress, we have investigated nitrogen doped bulk III-V compounds. In this article, a carbon–nitrogen defect in which the carbon–nitrogen bond is a triple bond is evidenced in GaP single crystals containing 10^{17} – 10^{18} cm^{-3} of nitrogen; as a matter of fact, carbon is a common p -type dopant in III-V-N dilute nitrides.⁴

II. EXPERIMENTAL DETAILS

The samples investigated in this study have been taken from bulk single crystals grown by the high-pressure (60 bar for GaP-based materials and 70 bar for GaAs-based materials) liquid encapsulation Czochralski technique using N_2 working gas; this working gas is at the origin of the presence of nitrogen in the samples. The crystals are either intentionally undoped or doped with different transition metal impurities, pinning the Fermi-level at different positions within the gap.

The absorption measurements in the near infrared region have been performed with either a Bruker IFS 120 HR or a Bomem DA3+ Fourier-transform spectrometer equipped with KBr beam splitters and cooled InSb detectors. The unapodized resolutions used were between 0.04 and 0.2 cm^{-1} . The spectra in the 480 – 620 cm^{-1} range were measured with a DTGS detector. The samples were investigated in the temperature range from 7 to 300 K mounted in Oxford Instruments optical cryostats.

Experiments with uniaxial stress were carried out using a home-made push rod apparatus inserted inside one of the cryostats. The oriented samples for the uniaxial stress experiments have the dimensions $2 \times 4 \times 10 \text{ mm}^3$ with the long edge along the three main crystallographic directions. The applied uniaxial stresses were less than 1° away from the $\langle 001 \rangle$, $\langle 111 \rangle$, and $\langle 110 \rangle$ directions.

III. RESULTS

A. Experiments without stress on GaP

In GaP samples, a sharp vibrational absorption line is measured at $T=7 \text{ K}$ located at 2087.12 cm^{-1} with a full width at half-maximum (FWHM) $\Gamma=0.06 \text{ cm}^{-1}$ (see Fig. 1). This line had been previously reported and assigned to a hydrogen related complex.⁵ However, experiments performed in samples doped with deuterium (see Ref. 6) ruled out this assignment, as in those samples no corresponding D -line could be detected. The results reported in this article confirm that the assignment proposed in Ref. 5 is not correct and allow the identification of the center responsible for this line. The line can be detected up to room temperature and the temperature dependences of its shift and FWHM shown in Fig. 2 confirm its vibrational nature. It has to be noted that these temperature dependences cannot be fitted with the standard model⁷ assuming anharmonic coupling with a low-frequency mode. The line shape is mostly Lorentzian at all temperatures.

Figure 3 shows the spectrum in the 480 – 620 cm^{-1} wave number range observed in a sample similar to that giving rise to the spectrum shown in Fig. 1. The line at 496.1 cm^{-1} is

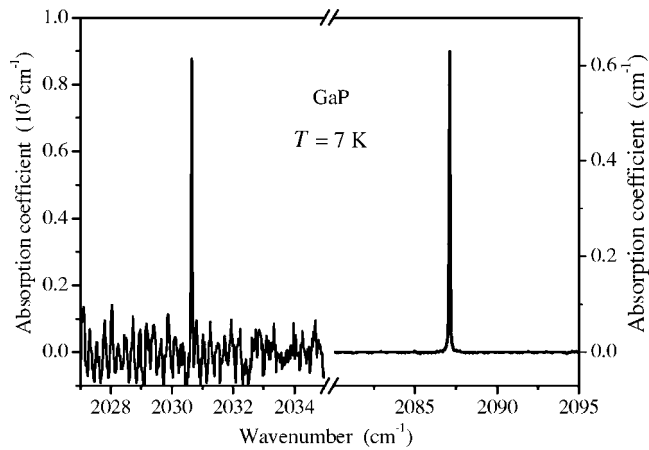


FIG. 1. Absorption spectrum of GaP measured at $T=7$ K with an unapodized resolution of 0.04 cm^{-1} . The line at 2087.12 cm^{-1} is due to the $^{12}\text{C}-^{14}\text{N}$ stretching mode, the line at 2030.66 cm^{-1} is due to the isotopically shifted $^{13}\text{C}-^{14}\text{N}$ mode.

due to the local vibrational mode (LVM) of nitrogen substituting phosphorus (N_p) and the line at 605.6 cm^{-1} is due to the LVM of carbon substituting phosphorus (C_p). The integrated intensities of both of these lines have been calibrated⁸⁻¹⁰ as a function of the $[N_p]$ and $[C_p]$ concentrations respectively; the C_p LVM calibrations were obtained^{9,10} by comparing the integrated intensity of the 605.6 cm^{-1} LVM with the concentration of compensated carbon acceptors and the N_p LVM calibration⁸ by correlating the integrated intensity of the 496.1 cm^{-1} LVM with the intensity of

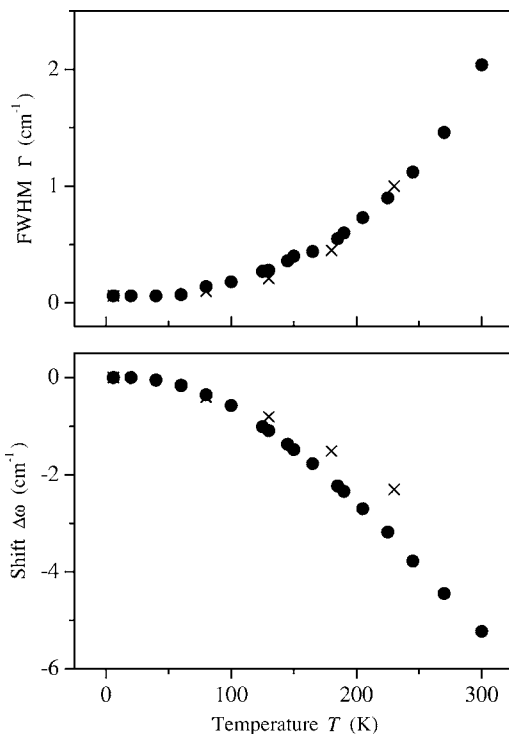


FIG. 2. Temperature dependence of the shift $\Delta\omega$ of the line position and FWHM Γ of the 2087.12 cm^{-1} line (circles). The crosses are the data points for the 2088.50 cm^{-1} line in GaAs.

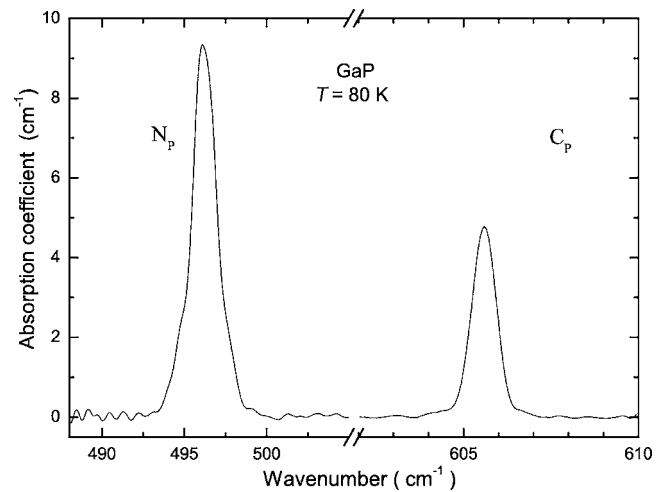


FIG. 3. Spectra of the local vibrational modes of substitutional nitrogen and substitutional carbon measured at $T=80$ K on a GaP sample; in that sample, $[N_p]=1.5 \times 10^{17}$ cm^{-3} and $[C_p]=3.7 \times 10^{16}$ cm^{-3} . The background due to the two-phonon absorption has been subtracted. The integrated intensity of the C—N stretching mode measured on this sample is $A^{2087}=2.3 \times 10^{-2}$ cm^{-2} (cf. Fig. 4).

the nitrogen bound exciton absorption line at $18\,638$ cm^{-1} . We used these calibration factors for determining $[N_p]$ and $[C_p]$ in the samples investigated in this study. It is important to note that the line at 2087.12 cm^{-1} can be observed only in GaP samples with substitutional carbon content $[C_p] > (1-5) \times 10^{16}$ cm^{-3} and nitrogen content $[N_p] > (1-2) \times 10^{17}$ cm^{-3} . In samples with lower content of C_p and N_p the line was not detectable. The Fermi level of the samples in which this line has been observed ranges from 0.3 eV above the top of the valence band to 0.8 eV below the bottom of the conduction band. The intensity of the line at 2087.12 cm^{-1} is unaffected by illumination of the samples with above or below band-gap light. This suggests that the center responsible of this vibrational mode can be present in only one charge state and therefore that it has no electronic level within the band gap.

Additionally, a weak line was measured at 2030.66 cm^{-1} ($\Gamma=0.05$ cm^{-1}) the integrated intensity A of which is correlated to that of the 2087.12 cm^{-1} line; this correlation is evidenced in Fig. 4. The intensity ratio $A^{2030}/A^{2087}=0.011$ corresponds exactly to the $[^{13}\text{C}]/[^{12}\text{C}]$ ratio of the natural abundances of the carbon isotopes. These results strongly suggest that the line at 2087.12 cm^{-1} is due to the stretching mode of a $^{12}\text{C}-^{14}\text{N}$ complex and the line at 2030.66 cm^{-1} is due to the isotopically shifted mode of the $^{13}\text{C}-^{14}\text{N}$ complex. The measured $^{12}\text{C}-^{13}\text{C}$ isotope shift $\Delta\omega=-56.5$ cm^{-1} is rather close to that calculated for a “free” C—N molecule in harmonic approximation (-43.7 cm^{-1}). In the sample in which the 2087.12 cm^{-1} line is the strongest, a line at 2048.45 cm^{-1} could be discerned with an integrated intensity about 0.003 times the integrated intensity of the 2087.12 cm^{-1} line; this corresponds to the ratio between the natural abundance of the nitrogen isotopes ($[^{15}\text{N}]/[^{14}\text{N}]=0.0036$). Moreover, the spacing $\Delta\omega=-38.67$ cm^{-1} between the 2048.45 and 2087.12 cm^{-1} lines is

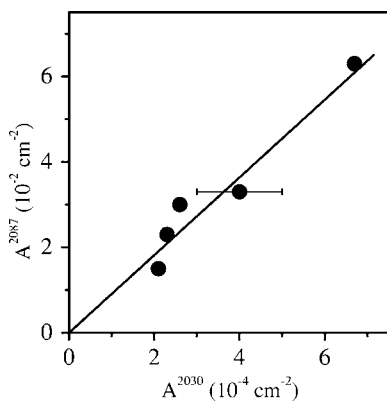


FIG. 4. Correlation between the integrated intensities A of the absorption lines at 2087.12 cm^{-1} and 2030.66 cm^{-1} . The straight line corresponds to the $[^{13}\text{C}]/[^{12}\text{C}]=0.011$ ratio of the carbon natural abundances.

close to the ^{15}N – ^{14}N isotope splitting expected for a “free” C–N molecule in harmonic approximation (-32.4 cm^{-1}). Therefore, we tentatively assign the line at 2048.45 cm^{-1} to the vibration of the ^{12}C – ^{15}N complex.

There are further arguments in favor of the assignment to a C–N complex. The C–N stretching frequency in gaseous HCN is 2097 cm^{-1} (Ref. 11) and the stretching mode of the C–N impurity on halogen sites in the chlorides and bromides of Na, K, and Rb are all within the narrow frequency region 2070 to 2100 cm^{-1} .¹²

It has to be noted that the integrated intensity of the 2087.12 cm^{-1} LVM is less than 1% of the ones of N_p and C_p . Even though we have no calibration factor for the 2087.12 cm^{-1} LVM, it can be stated that the concentration of the carbon–nitrogen complexes is much smaller than $[\text{N}_p]$ and $[\text{C}_p]$ in the samples investigated in this study.

B. Experiments under uniaxial stress on GaP

Experiments under uniaxial stress allow one to lift the orientational degeneracy of the complex and to determine its geometry.¹³ Experiments have been performed with uniaxial stress σ up to 220 MPa applied along the $\langle 001 \rangle$, $\langle 111 \rangle$, and $\langle 110 \rangle$ crystallographic directions using polarized light with its electric vector E parallel or perpendicular to the stress direction. Figure 5 shows the spectra obtained with polarized light for the highest stresses used. One sees that the line at 2087.12 cm^{-1} splits into two fully polarized components having equal integrated intensities for stress $\sigma \parallel \langle 001 \rangle$ and $\parallel \langle 110 \rangle$, and is only shifted to higher frequencies for $\sigma \parallel \langle 111 \rangle$. Figure 6 shows the shifts and splittings of the lines as a function of the applied stress. There is a broadening of the lines due to the imperfection of the applied uniaxial stress that can be seen comparing Figs. 1 and 5; for the largest applied stress, the LVMs are broadest. That is why the error bars, that have been taken equal to the FWHM, increase with the stress in Fig. 6. This behavior under uniaxial stress is exactly the one, given in Table I, expected for a nondegenerate mode of a complex aligned along one of the tetragonal S_4 axes of the lattice.¹⁴ It clearly indicates that the induced

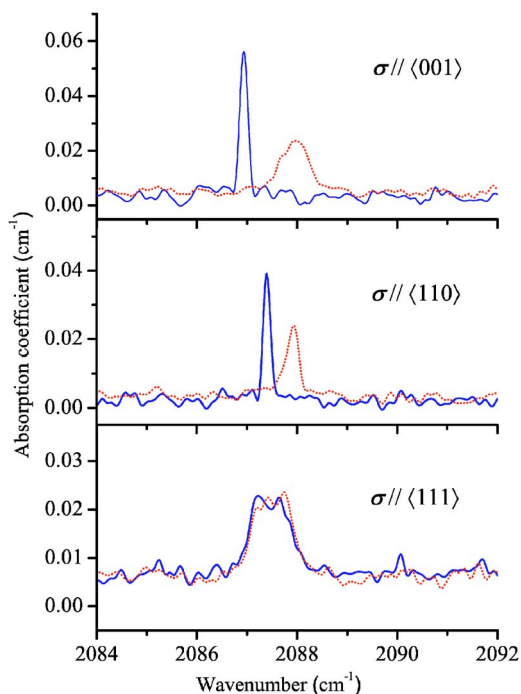


FIG. 5. (Color online) Spectra in GaP under uniaxial stress. The full line spectra correspond to the polarization parallel to the stress and the dotted line ones to the polarization perpendicular to the stress. $\sigma=210\text{ MPa}$ for $\sigma \parallel \langle 001 \rangle$ and $\sigma \parallel \langle 111 \rangle$; $\sigma=230\text{ MPa}$ for $\sigma \parallel \langle 110 \rangle$.

dipole moment of the C–N stretching mode is oriented along one of the three equivalent $\langle 001 \rangle$ directions. The straight lines in Fig. 6 are the fully consistent fit with the parameters that are defined in Table I: $A_1=-0.9\text{ cm}^{-1}/\text{GPa}$ and $A_2=3.4\text{ cm}^{-1}/\text{GPa}$, compressive stress being considered as positive. No stress-induced dichroism was observed when a stress $\sigma=150\text{ MPa}$ was applied parallel to the $\langle 001 \rangle$ direction at $T=300\text{ K}$, cooled down under stress, and measured at $T=7\text{ K}$ after releasing the stress (cf. Ref. 13). Therefore, no thermal reorientation between the three $\langle 100 \rangle$ directions is possible at $T=300\text{ K}$; the activation energy for this reorientation is therefore larger than 1 eV.

C. Experiments without stress on GaAs

In a GaAs sample containing $[\text{C}_{\text{As}}]=5 \times 10^{15}\text{ cm}^{-3}$ and $[\text{N}_{\text{As}}]=2 \times 10^{16}\text{ cm}^{-3}$, a weak vibrational absorption line was measured at 2088.50 cm^{-1} ($\Gamma=0.06\text{ cm}^{-1}$). This line is possibly due to the stretching mode of the ^{12}C – ^{14}N complex in GaAs because of the nearly identical vibrational frequency as well as similar temperature dependences as in GaP (cf. Fig. 2).

IV. DISCUSSION

As the stretching frequency is very close to that of triply bonded C–N in molecules, the C–N bond length is as small as about 0.12 nm (Ref. 11) also in GaP and GaAs. The formation of the C–N defect is favored, because the triple C–N bond is known to be very strong and therefore its

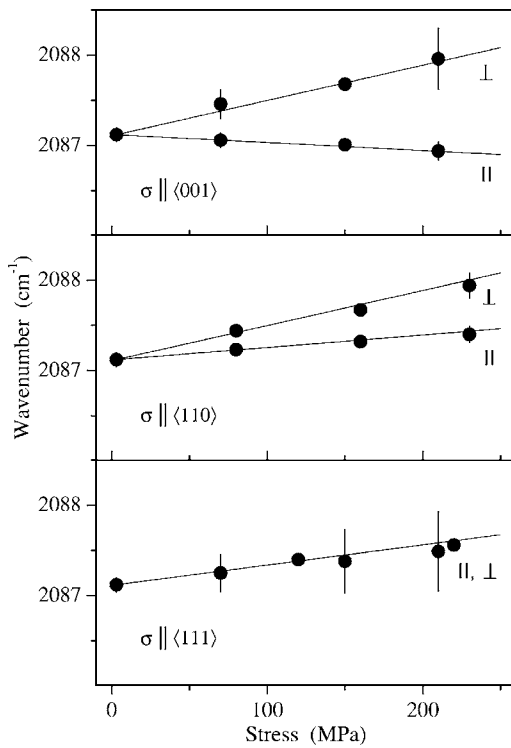


FIG. 6. Effects of uniaxial stress applied along $\langle 001 \rangle$, $\langle 110 \rangle$, and $\langle 111 \rangle$ lattice directions on the vibrational line at 2087.12 cm^{-1} . The circles are the measured positions of the split components, the used unapodized resolution is 0.2 cm^{-1} . The sticks indicate the half-widths of the lines. \parallel means that the line is observed with the electric vector \mathbf{E} of the polarized light parallel to the stress direction $\boldsymbol{\sigma}$, \perp means, that the line is observed for \mathbf{E} perpendicular to $\boldsymbol{\sigma}$. The solid lines are the fit with the tetragonal splitting parameters A_1 and A_2 given in the text.

formation reduces the total energy of the crystal. Defects aligned along $\langle 001 \rangle$ axes are unusual in III-V compounds; most of the defects observed in these compounds are trigonal or have a lower symmetry. As far as symmetry is concerned, the experimental results reported in this paper offer the following possibilities for the structure of the complex in GaP: (i) C—N at a substitutional site, and (ii) C—N at a tetrahedral interstitial site. Figure 7(a) represents schematically

TABLE I. Stress-induced splittings for a nondegenerate vibrational mode of a complex aligned along one of the S_4 axes of the GaP lattice. ω_0 is the frequency at zero stress, σ is the magnitude of the stress; A_1 and A_2 , are fitting parameters. I_{\parallel} and I_{\perp} are the relative intensities of the lines with polarizations parallel and perpendicular to the stress direction respectively; for $\boldsymbol{\sigma} \parallel [110]$ the perpendicular polarization is parallel to the $[001]$ axis.

Direction of stress	Frequency	I_{\parallel}	I_{\perp}
$\langle 001 \rangle$	$\omega_0 + A_1 \sigma$	1	0
	$\omega_0 + A_2 \sigma$	0	1
$\langle 111 \rangle$	$\omega_0 + (1/3)(A_1 + 2A_2)\sigma$	1	1
$\langle 110 \rangle$	$\omega_0 + (1/2)(A_1 + A_2)\sigma$	1	0
	$\omega_0 + A_2 \sigma$	0	1

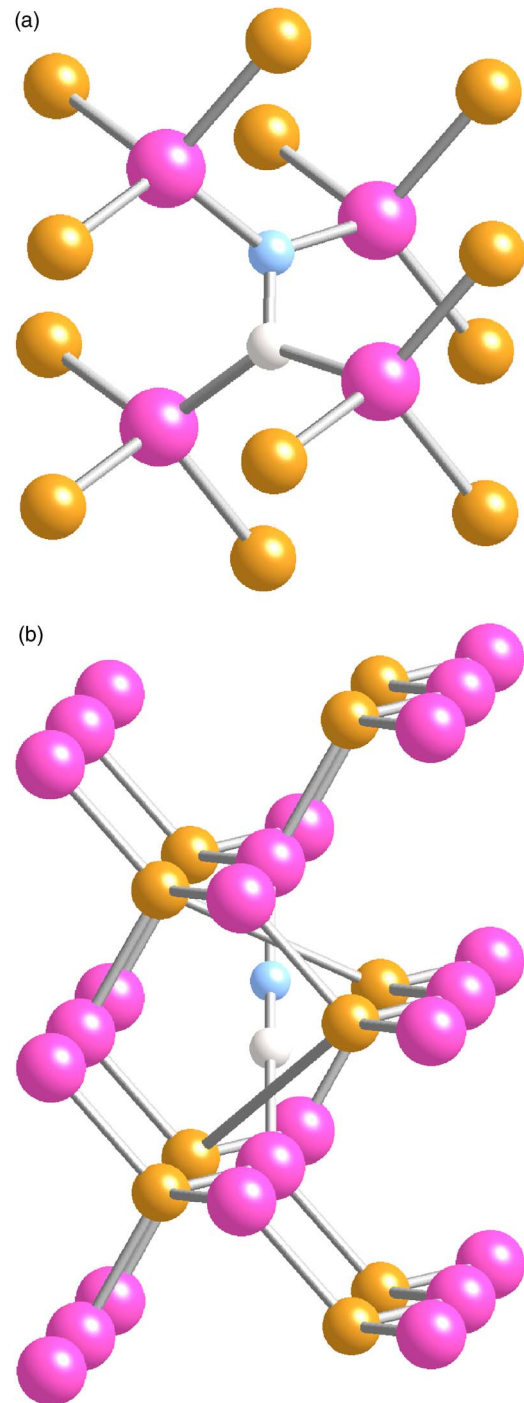


FIG. 7. (Color online) Ball and stick schematic representation of (a) a C—N radical substituting a phosphorus atom and (b) a C—N radical in a T_p interstitial site. The largest balls are gallium atoms, the intermediate size ones phosphorus atoms, and the two small balls the carbon and nitrogen atoms. The relaxation of the host atoms has not been represented.

C—N substitutional to a phosphorus atom and Fig. 7(b) C—N at a tetrahedral T_p site in which C—N has four phosphorus nearest neighbors. In both cases, the C—N bonds are aligned along fourfold axes of the host and the symmetry is C_{2v} . In the substitutional site configuration, both the carbon and nitrogen atoms are sp^2 hybridized. Their nonhybridized

p orbitals, which are perpendicular to the three bonds of the atom, are perpendicular to each other and cannot make a π bond. In this configuration, the C—N bond is therefore single bond like. This leads rejecting this possibility because it should give a clearly smaller vibration wave number, in the range 900–1200 cm^{-1} , than the one observed experimentally. C—N substitutional to a gallium atom would have the same drawback and moreover would be energetically less favorable. In the interstitial configuration represented in Fig. 7(b), the carbon and nitrogen atoms are sp hybridized. In this configuration, the C—N bond is triple-bond-like and therefore has a wave number compatible with the one measured. As a matter of fact, if one adds typical bondlengths of a Ga—N bond (about 0.2 nm), C—N triple bond (about 0.12 nm), and Ga—C (about 0.2 nm), one obtains a value comparable with the GaP lattice constant (0.545 nm); this makes the proposed structure quite plausible. Of importance in the structure of the complex is the reconstruction of the bonds around the T_p site; i.e., the rebonding of the phosphorus atoms schematized in Fig. 7(b). Of course there should be some relaxation of the atoms not represented in Fig. 7(b). C—N in a T_{Ga} tetragonal interstitial site, in which the complex has four gallium nearest neighbors, would be energetically less favorable than in a T_p site for two reasons. Firstly, carbon and nitrogen atoms prefer to sit in group-V sites in GaP and GaAs, which means that they prefer being bonded to gallium atoms, as in the complex shown in Fig. 7(b), rather than to phosphorous atom as would be the case if the C—N complex was in a T_{Ga} site. Secondly, the rebonding of the four phosphorus atoms nearest neighbors to the complex in a T_p site brings more energy than the rebonding of the four gallium atom nearest neighbors to the complex in a T_{Ga} site would as, in gaseous phase, the P—P and Ga—Ga bond energies are, respectively, 489 kJ mole^{-1} and 112 kJ mole^{-1} . Therefore, we believe that the most plausible structure for the C—N complex in GaP is C—N at a T_p site schematized in Fig. 7(b). Of course, this structure needs to be confirmed theoretically. The nonreorientation of the complex at room temperature is easily understandable as it necessitates the breaking of a Ga—C bond, a Ga—N bond, and the two P—P reconstructed bonds before the rearrangement and rebonding of other equivalent atoms; therefore, the potential energy barrier between equivalent configurations of the complex should be quite high. This structure of the complex could also explain the fact that the model⁷ involving anharmonic coupling with a single low-frequency mode does not work in explaining the behavior of the LVM with temperature both in GaP and GaAs: as the C—H radical is linked to the lattice by the Ga—C and Ga—N bonds, a model involving the coupling to two low-frequency modes would be more appropriate.

It has to be noted that the use of nitrogen doped bulk single crystals are essential for the investigation reported in this article. Experiments under uniaxial stress that allow one to assess the structure of the complex would have been im-

possible with conventional heteroepitaxial dilute nitrides; moreover, the observation of the isotopic shifts, which allows the determination of the chemical species involved in the complex, would probably not be observable in the standard dilute nitride layers. The carbon atoms that are involved in the complex reported here do not play their expected role of shallow p -type dopant as it seems, at least in GaP, that the complexes are electrically inactive.

The nitrogen concentration in the samples investigated in this study is in the range 10^{17} – 10^{18} cm^{-3} . A most important question is to determine whether the C—N complexes reported here are also present in carbon-doped dilute nitrides in which the nitrogen concentration is 100–1000 times higher. Even though we have no quantitative estimate of the C—N complexes concentration in our samples, it is clear that it is higher than it would be if the complexes were statistically formed, in which case it would be in the 10^{12} cm^{-3} range. This is due to the fact that the very high energy of the triple C—N bond favors the formation of such complexes in order to minimize the energy of the crystal. Therefore, in samples in which the nitrogen concentration is higher by several orders of magnitude than in samples investigated in this study, we expect the percentage of the carbon atoms involved in C—N complexes to be higher than in the samples investigated here. Therefore, we expect these complexes to be present in noticeable concentration in carbon-doped GaAs—N dilute nitride. Unfortunately, we do not yet have such samples available for checking this important point.

This type of triply bonded C—N complexes might also be present in nitrides such as GaN grown by organometallic vapor phase epitaxy, carbon being a residual impurity coming from the precursors. It should be of interest to look for vibrational modes around 2100 cm^{-1} in these materials for evidencing such complexes.

V. SUMMARY

In this article, we have demonstrated the formation of C—N complexes in GaP. In these complexes, the C—N triple bond is aligned along one of the fourfold axes of the lattice. It is proposed that C—N sits in a tetrahedral T_p interstitial site in GaP. Arguments for the existence of the same type of complex in GaAs are presented. The carbon atoms involved in these complexes do not contribute to the p -type doping of the samples. These complexes are expected to form in GaP—N and GaAs—N dilute nitrides. Therefore, even though carbon is the most commonly used p -type dopant in GaAs, it might not be the ideal dopant in GaAs—N dilute nitride.

ACKNOWLEDGMENTS

The authors thank C. Naud for his help with the stress experiments and for helpful discussions, H. v. Kiedrowski for the preparation of the oriented samples and B. Pajot, and L. Siozade for helpful discussions.

- ¹R. J. Potter and N. Balkan, *J. Phys.: Condens. Matter* **16**, S3387 (2004).
- ²H. Yonezu, *Semicond. Sci. Technol.* **17**, 762 (2002).
- ³I. A. Buyanova, W. M. Chen, and C. W. Tu, *J. Phys.: Condens. Matter* **16**, S3027 (2004).
- ⁴R. E. Welsler, R. S. Setzko, K. S. Stevens, E. M. Rehder, C. R. Lutz, D. S. Hill, and P. J. Zarnparadi, *J. Phys.: Condens. Matter* **16**, S3373 (2004).
- ⁵B. Clerjoud, D. Côte, and W. S. Hahn, *Mater. Sci. Forum* **148–149**, 281 (1994).
- ⁶W. Ulrici and M. Jurisch, *Phys. Status Solidi B* **233**, 263 (2002).
- ⁷B. N. J. Persson and R. Ryberg, *Phys. Rev. B* **32**, 3586 (1985).
- ⁸W. Ulrici and M. Czupalla, *Phys. Status Solidi B* **223**, 613 (2001).
- ⁹F. Thompson and R. C. Newman, *J. Phys. C* **4**, 3249 (1971).
- ¹⁰E. G. Grosche, R. C. Newman, D. A. Robbie, R. S. Leigh, and M. J. L. Sangster, *Phys. Rev. B* **56**, 15701 (1997).
- ¹¹G. Herzberg, in *Molecular Spectra and Molecular Structure II. Infrared and Raman Spectra of Polyatomic Molecules* (Krieger, Malabar, FL, 1991).
- ¹²W. D. Seward and V. Narayanamurti, *Phys. Rev.* **148**, 463 (1966).
- ¹³M. Stavola, *Semicond. Semimetals* **51 B**, 153 (1999).
- ¹⁴A. A. Kaplyanskii, *Opt. Spektrosk.* **16**, 602 (1964) [*Opt. Spectrosc.* **16**, 329 (1964)].